Beamspace MIMO-NOMA for Millimeter-Wave Broadcasting via Full-Duplex D2D Communications

Jianguo Li, Xiangming Li, *Member, IEEE*, Aihua Wang, *Member, IEEE*, and Neng Ye

***Abstract*—In order to meet the tremendous requirements on the convergence between broadband and broadcast, this paper proposes to incorporate layered division multiplexing (LDM), an important variant of non-orthogonal multiple access (NOMA) technologies, into Millimeter wave (mmWave) multiple-input multiple-output (MIMO) system with device-to-device (D2D) communications to simultaneously provide broadcast and unicast services. The performance of the proposed full-duplex D2D-aided mmWave MIMO-NOMA with randomly deployed users is then analyzed under practical assumptions. Closed-form expressions of both the outage probability and the ergodic capacity are then derived by using the Laplace transform technique. Finally, detailed numerical results reveal the performance gains of the proposed scheme compared with the LDM without D2D communications and conventional time division multiplexing based scheme. The impacts of the antenna array gain and the transmission power of both the base station and the full-duplex link on system performance are also presented. Besides, we observe that it is vital to optimal the transmission power of the full-duplex link which ensures less self-interference to enhance the system capacity.**

***Index Terms*—Outage probability, ergodic capacity, LDM, MIMO, full-duplex D2D communications.**

I. Introduction

With the explosive growth of a variety of the commercial broadband and broadcast services, the demands on high data rate, high spectral efficiency and low latency wireless communications system also increase rapidly. To simultaneously achieve high data throughput, high environmental adaptability, and high physical resource utilization in broadcast network, the Advanced Television Systems Committee (ATSC) has standardized the physical layer specification of ATSC 3.0 system for diversified requirements of the market and target devices [1]–[3]. With the adjustable operating mode, ATSC 3.0 can achieve a goal to balance cellular coverage and system throughput. In addition, the advantages of broadcast and unicast are combined by the cellular network to optimize the system for delivering the broadcast services [4]. The LTE-Advanced Pro has provided the point-to-multipoint transmission by vehicular to everything, Internet of Things and machine-type communication. In 2019, the study on the 5G multicast-broadcast services has been agreed by the 3rd Generation Partnership Project (3GPP) in the future releases of 5G [5].

The power based layered division multiplexing (LDM) is a non-orthogonal technology whose transmitted signal consists of two different layers [6], and the power of each layer is different. In this case, the robust layer can be used to transmit broadcast signals, and the large capactiy layer can be adoped to transmit unicast signal. LDM is a promising technology for the integration of broadband and broadcast [7], [8]. Different from the time division multiplexing (TDM) and frequency division multiplexing (FDM), LDM multiplexes unicast transmission and broadcast transmission in a non-orthogonal fashion to simultaneously achieve high spectrum efficiency and large coverage [9]–[13]. Considering the diversified Quality of Service (QoS) requirements of the multiplexed services, LDM supports to choose different transmission power, channel coding and modulation schemes for different layers [14]. In addition, the authors in [15] have proposed a novel low complexity LDM structures for the next generation terrestrial broadcasting systems which can achieve a significant performance gain compared to conventional TDM. Additionally, the N-layered theoretical capacity and the new application scenarios have been introduced in the literature [16]. Furthermore, the performance of LDM with a wide range of stationary channels and the mobile TU-6 channel has been introduced based on the software defined radio platform in the literature [17]. According to the literature [18], the LDM technology has been proposed to improve the LTE evolved multimedia broadcast multicast services (eMBMS). The authors in [19] have shown the performance advantages and potential usage scenarios of combing LDM with multi-radio-frequency channel technologies which can deliver the serves data across two or more radio frequency channels by time slicing and frequency hopping.

D2D communication has been considered as the preferred solution for the content sharing, proximity services and coverage expansion with business purposes in the 3GPP LTE

Manuscript received November 30, 2019; revised February 8, 2020; accepted February 12, 2020. Date of publication March 12, 2020; date of current version June 5, 2020. This work was supported in part by the National Nature Science Foundation of China under Grant 61771051 and Grant 61620106001, and in part by the Advance Research Projects of 13th Five-Year Plan of Civil Aerospace Technology under Grant B0105. *(Corresponding author: Xiangming Li.)*

The authors are with the School of Information and Electronics, Beijing Institute of Technology, Beijing 100081, China (e-mail: jianguoli@bit.edu.cn; xmli@bit.edu.cn; wah@bit.edu.cn; ianye@bit.edu.cn).

Color versions of one or more of the figures in this article are available online at http://ieeexplore.ieee.org.

Digital Object Identifier 10.1109/TBC.2020.2977576

Release 12 and 13. D2D communication allows a pair of users with closed geographical distances to communicate directly without going though the base station. In the mean time, full-duplex technology is a promising technology to double the spectral efficiency by simultaneous transmission and reception at the same time and the frequency. This feature of full-duplex can be taken advantage at the relay nodes in D2D communication to decrease the time consumption [20]. Since the same time-frequency resources are utilized by the cellular users and D2D users, the power control has been one focus of researchers in recent years. In the literature [21], the centralized and distributed power control themes of the incorporating full-duplex D2D cellular network have been proposed. The self-reference signal of the full-duplex relaying system has been analyzed in [22]–[24]. And the closed-form approximations of cellular and D2D coverage probabilities have been derived. Meanwhile, the cooperative full-duplex D2D aided cellular network has been introduced in [25] where the cellular user supports D2D communication as a full-duplex relay and an optimal power allocation scheme has been investigated to maximize the system throughout. Moreover, a closed-form expression for the optimal power allocation scheme in the wireless cellular network with full duplex D2D communications has been obtained in the literature [26]. In the literature [27], the bottle-neck effect elimination power algorithm has been proposed to boost the energy efficiency of the full-duplex relay-adided mmWave D2D communications. Furthermore, the literature [28] has proposed a cooperative sub-channel allocation approach in the mmWave networks with D2D communications to improve the resource utilization and network capacity. In addition, the authors in [29] has studied relay-assisted D2D communication in mmWave based 5G networks to balances the trade-off between transmit power and system throughput.

With the increasing demand for a variety of applications and increasingly tight spectrum resources, mmWave has become the optimal choice for high speed, low latency and high throughput communication systems. Due to the large attenuation of the mmWave link, a large scale antenna array is required to improve the antenna gain to ensure the QoS [30]. Furthermore, thanks to the recent development of the antenna circuit design, it is possible to realize large scale antenna arrays including 32 to 256 antennas [31]. The mmWave transceiver architectures are composed of fully digital architecture, analog-only architecture and hybrid analog/digital architecture. In addition, the authors in the literature [32] have proposed a 64-channel massive MIMO transceiver with a fully digital beamforming architecture for mmWave communication which can achieve a downlink data rate of 50.73 Gb/s with 101.5 b/s/Hz. However, because of the high cost and power consumption of high resolution analog to digital converters, it is difficult to realize the fully digital processing at mmWave frequencies with wide bandwidths and large antenna arrays [33]–[35]. Moreover, analog-only architectures are easy to implement by using the phase shifters. However due to the characteristics of phase shifters, it is difficult to generate multi-beams or support multi-users MIMO communication. Meanwhile, the energy-efficient analog beamforming in mmWave multicast transmission has been proposed in the literature [36] which can realize the optimal beamformer designs and provide asymptotic performance analysis for mmWave multicasting systems. Furthermore, the beamspace MIMO-NOMA for mmWave communications using lens antenna arrays has been investigated in the literature [37], which can achieves a higher spectrum and energy efficiency than the existing system. And the partially-connected hybrid pre-coding design method has been proposed in the literature [38] to maximize the weighted sum of channel gains for mmWave MIMO broadcast channels.

The beamspace MIMO-NOMA and full-duplex D2D communications can be combined to enhance the coverage of broadcast and improve the throughout of unicast in the mmWave broadcasting network. Nonetheless, few researches have analysed the system performance. In this paper, we propose a full-duplex D2D-aided mmWave MIMO-NOMA broadcasting network. Then we analyse the performance of the proposed system under the practical assumptions such as directional beamforming, distanc-dependent pathloss and self-interference of full-duplex communication. The closed-form formulation of the outage probability and the ergodic capacity are derived with Laplace transform technique. Finally, the numerical results indicate that the LDM outperforms the TDM. And the impacts of the antenna array gain and the transmission powers of both base station and the full-duplex link are considered.

The rest of this paper is organized as follows. In Section II, we introduce a system model of the beamspace MIMO-NOMA for mmWave broadcasting via full-duplex D2D communications. The closed-form expressions of the performance analysis including the outage probability and the ergodic capacity is given in Section III. Finally, the numerical results in Section IV validate the theoretical analysis and demonstrate that the system capacity can be improved by the LDM.

II. System Model

The paper considers a full-duplex D2D-aided mmWave beamspace MIMO-NOMA system for broadcast and unicast, as shown in Fig. 1. The system consists of one base station and Q cellular users which are randomly and uniformly distributed in the cellular network. The base station is equipped with multiple antennas to generate multiple beams with the beamspace methods for cellular users. There are Q cellular user with signal antenna in the cellular network which is denoted as $CU_1, CU_2, \ldots, CU_Q$. The cellular users randomly in one beam are paired and communicate with the LDM. In addition, in order to reduce the system complexity, we only consider one beam in the proposed system. There are two users in this beam which are denoted as near user and far user by their distance to the base station. The near user receivers the broadcast and unicast signal of the base station, while the far user receiving the broadcast signal from base station and near user. Due to the great attenuation of the millimeter wave system, it is assumed that the near user can provide additional services to the far user through the D2D link with a full-duplex relay.

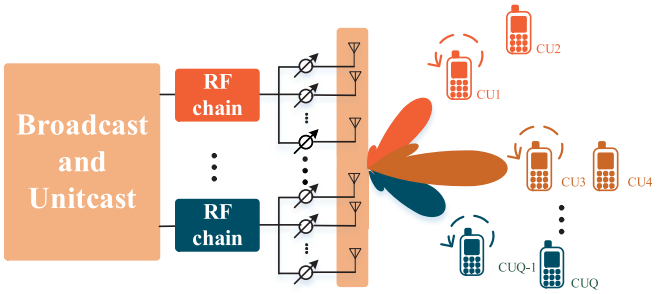

Fig. 1. System model of full-duplex D2D-aided mmWave MIMO-NOMA for broadcast and unicast.

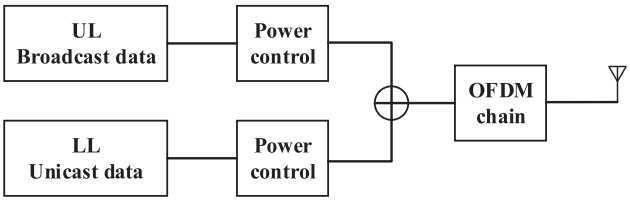

Fig. 2. Two-layer LDM transmitter.

A. Layered Division Multiplexing

In order to improve the spectrum efficiency, the two-layer LDM structure was proposed by the ATSC 3.0 to deliver reliable mobile TV services for a large variety of mobile and indoor users. To incorporate LDM in mmWave system, the same mmWave resources are used by the cellular users with the two-layer LDM structure where different layer provides different services. In addition, the upper layer (UL) signal is adopted to deliver reliable mobile broadcast services and the lower layer (LL) signal is designed to deliver the unicast services. The system diagrams of the transmitter in the two-layer LDM is shown in the Fig. 2. The signal for each layer is generated by a separate module, and the signals are superimposed and transmitted in the form of the OFDM data link. According to the high coverage of the broadcast signal and the high data rate of the unicast signal, high power transmission is adopted by the UL signal, and the LL signal is transmitted with lower power.

In n-th beam, the UL,LL in the n-th beam is denoted as $UL(n), LL(n)$. We assume that $UL(n), LL(n)$ are scheduled on the same radio resource with LDM. We denote x_n as the composite transmission signal of the base station in the n-th beam, which is given by

$$x_n = \sqrt{\lambda_{UL(n)} P_n} S_{UL(n)} + \sqrt{\lambda_{LL(n)} P_n} S_{LL(n)}, \tag{1}$$

where $\lambda_{UL(n)}$ and $\lambda_{LL(n)}$ are the power coefficients of UL and LL, respectably, satisfying $\lambda_{UL(n)} + \lambda_{LL(n)} = 1$ and $\lambda_{UL(n)} > \lambda_{LL(n)}$. P_n is the total power in the n-th beam, $S_{UL(n)}, S_{LL(n)}$ is the normalized transmission signal of UL and LL in the n-th beam with $\mathbb{E}(\|S_{UL(n)}\|^2) = \mathbb{E}(\|S_{LL(n)}\|^2) = 1$.

B. Channel Model

The experimental investigations have shown that the mmWave channel is sensitive to the blockage effects. Different channel statistics are proposed by the 3GPP for LOS and NLOS links in the simulation. Therefore the rectangle Boolean stochastic blockage model is used to model building blockages by differentiating the LOS and NLOS link [39]. The probability function of a LOS link is denoted as

$$P_L(r) = \exp(-\beta r), \tag{2}$$

where r is the distance from transmitter to receiver, β is used to describe the size and density of blockages. And the probability function of a NLOS link is $P_N = 1 - \exp(-\beta r)$. Without loss of generality, we assume that the probability function of LOS with different link is independent.

Depending on the Friis equation [33], the mmWave can not propagate well in free space. The large scale fading $L(r)$ in dB of the mmWave link ,which is introduced in [40], is modeled as

$$L(r) = 32.4 + 20\log(f_c) + 10\alpha\log(r), \tag{3}$$

where f_c is the carrier frequency, $\alpha \in \{\alpha_L, \alpha_N\}$ is the path loss exponents of LOS, NLOS, and r is the distance between the transmitter and receiver.

As for the small scale fading, we assume that each link between the transmitter and receiver is Nakagami-m fading [41]. h_{u_1}, h_{u_2}, h_{I_1} and h_D are denoted as the link of the base station to the near user, the base station to the far user, the near user to the near user and the near user to the far user. Without loss of generality, we assume that $\|h_{u_1}\|^2$, $\|h_{u_2}\|^2$ and $\|h_D\|^2$ follow the normalized Gamma random varible with $N \in \{N_L, N_N\}$ which is the parameter of LOS link or NLOS link. Then the h_{I_1} is free of fading. And the probability density function $f(x)$ and the cumulative distribution function $F(x)$ of $\|h_{u_1}\|^2$ are respectively given by

$$f(x) = \frac{N^N}{\Gamma(N)} x^{N-1} e^{-Nx}, \tag{4}$$

and

$$F(x) = \begin{cases} 1 - \sum_{J=0}^{N-1} \frac{N^j}{j!} x^j e^{-Nx}, & x \geq 0 \\ 0, & \text{otherwise.} \end{cases} \tag{5}$$

C. Large Antenna Arrays

Due to the large attenuation of the mmWave link, the high gain and high directional beam is generated by the base station to ensure high QoS. To simplify the mathematical analysis, we assume the actual antenna model as the sectorized antenna model which means the array gain within the half-power beam width (main lobe gain) is replaced by the maximum power gain and the other direction of arrivals (side lobe gain) is replaced by the first minor maximum gain. Then the total array gain $G(n)$ is denoted as [42],

$$G(n) = \begin{cases} \Psi, & \textit{main lobe} \\ \psi, & \textit{side lobe}, \end{cases} \tag{6}$$

where $\Psi = M$, $\psi = 1/sin^2(\frac{3\pi}{2\sqrt{M}})$ and M is the number of antennas.

D. Receive Signal

For the broadcast and unicast transmissions, not only receiving the signal from the base station, the near user but also receives the self-interference signal by itself due to the full duplex. Meanwhile, the far user receives the broadcast data from the base station and the near user. Without loss of generality, the near user and far user in one beam are introduced as followed. Then the received signal of near user y_{u1} and the received signal of far user y_{u2} can be respectively formulated as

$$y_{u1} = \frac{h_{u1}G(n)x_n}{L(d_1)} + \frac{h_{I_1}\sqrt{P_D}S_{UL}}{L_{I_1}} + n_{u1}, \tag{7}$$

and

$$y_{u2} = \frac{h_{u2}G(n)x_n}{L(d_2)} + \frac{h_D\sqrt{P_D}S_{UL}}{L(d_2-d_1)} + n_{u2}, \tag{8}$$

where h_{u1}, h_{u2} is the channel gain from the base station to the near user and the far user respectively, $\|h_{u1}\|^2 > \|h_{u2}\|^2$. h_{I_1} is the channel gain from the near user to the near user. h_D is the channel gain from the near user to the far user. x_n is the superimposed signal by the broadcast and unicast data in the n-th beam. d_1, d_2 are the distance from base station to the near user and far user. In addition, the distance between the two users is approximated by the difference between their distance to the base station due to the narrow beam width of mmWave. L_{I_1} is the self-interference signal link attenuation of near user. P_D is the transmitted power from near user to far user. S_{UL} is the broadcast signal from the near user to the far user, $\mathbb{E}(\|S_{UL(n)}\|^2) = 1$. In addition, n_{u1}, n_{u2} are the independent and identically distributed normalized white Gaussian noise which are denoted as $n_{u1}, n_{u2} \sim \mathcal{CN}(0, 1)$.

III. Performance Analysis

In this section, the performance analysis of full-duplex D2D-aided mmWave beamspace MIMO-NOMA is proposed. The outage probability of users and the ergodic capacities of broadcast and unicast services are introduced as followed. In the proposed system, firstly, the base station transmits the LDM signal to the cellular users. Next, the near user receives the broadcast and unicast signal with the perfect successive interference cancellation method. Then the full-duplex mode with D2D communication is adopted to transmit broadcast signals to far user. Finally, the far user receives the signals from the base station and the D2D links. Two events are considered in the system as followed.

Event 1: The received signal of the near user is described as event one. The near user receives the signal sent by the base station and the self-interference signal of the near user. The broadcast signal is first solved by regarding the unicast signal and the self-interference signal as interference. Then the near user cancels the broadcast signal and resolves the unicast signal in the presence of self-interference signals. The near user first decodes the broadcast data and remove it with γ_{B1} and then the near user obtains the unicast data with γ_{U1}.

$$\gamma_{B1} = \frac{\lambda_{UL(n)}G(n)P_n/L(d_1)\|h_{u1}\|^2}{\lambda_{LL(n)}G(n)P_n/L(d_1)\|h_{u1}\|^2 + P_D/L_{I_1}\left\|h_{I_1}\right\|^2 + \sigma_1^2}, \tag{9}$$

$$\gamma_{U1} = \frac{\lambda_{LL(n)}G(n)P_n/L(d_1)\|h_{u1}\|^2}{P_D/L_{I_1}\left\|h_{I_1}\right\|^2 + \sigma_1^2}. \tag{10}$$

Event 2: The received signal of the far user is described as event two. The far user receives the broadcast data from the base station and the near user at the same time. We assume that these two signals are solvable at far user, so that the maximal ratio combing method can be adopted. Therefore, the far user can acquire the broadcast data with γ_{B2}.

$$\gamma_{B2} = \frac{\lambda_{UL(n)}G(n)P_n/L(d_2)\|h_{u2}\|^2 + P_D/L(d_2-d_1)\left\|h_{I_D}\right\|^2}{\lambda_{LL(n)}G(n)P_n/L(d_2)\|h_{u2}\|^2 + \sigma_2^2}. \tag{11}$$

A. Outage Probability

The outage probability of near user and far user is considered in this part. The target rate of the broadcast of near user, unicast of near user and broadcast of far user are denoted as R_1, R_2 and R_3, respectively. And the outage probability of near user and far user are denoted as P_1 and P_2 as follows,

$$\begin{aligned} P_1 &= P(\log(1+\gamma_{B1}) < R_1 \ or \ \log(1+\gamma_{U1}) < R_2) \\ &= 1 - P(\log(1+\gamma_{B1}) \geq R_1)P(\log(1+\gamma_{U1}) \geq R_2), \end{aligned} \tag{12}$$

$$P_2 = P(\log(1+\gamma_{B2}) < R_3). \tag{13}$$

First of all, we consider the term $P(\log(1+\gamma_{B1}) < R_1)$. By denoting $\epsilon_1 = 2^{R_1} - 1$, this term can be formulated as

$$\begin{aligned} &P(\log(1+\gamma_{B1}) < R_1) \\ &= P\left(\frac{\lambda_{UL(n)}P_nG(n)/L(d_1)\|h_{u1}\|^2}{\frac{\lambda_{LL(n)}P_nG(n)}{L(d_1)}\|h_{u1}\|^2 + P_D/L_{I_1}\left\|h_{I_1}\right\|^2 + \sigma_1^2} < \epsilon_1\right). \end{aligned} \tag{14}$$

Then we denote $\eta = \frac{\epsilon_1 L(d_1)N_m}{(\lambda_{UL(n)} - \lambda_{LL(n)}\epsilon_1)P_nG(n)}$, $I_1 = \frac{P_D\|h_{I_1}\|^2}{L_{I_1}}$, $\|h_{u1}\|^2 \sim Gamma(N_m), N_m \in \{N_L, N_N\}$. When the $\eta \leq 0$, the (14) is equal to 1. Otherwise, the (14) can be simplified to

$$\begin{aligned} &P\left(\|h_{u1}\|^2 < \frac{\eta}{N_m}\left(I_1 + \sigma_1^2\right)\right) \\ &= \mathbb{E}_{d_1}\left\{P\left(\|h_{u1}\|^2 < \frac{\eta}{N_m}\left(I_1 + \sigma_1^2\right)\right)|d_1\right\} \\ &= \mathbb{E}_{d_1}\left\{\sum_{m\in\{L,N\}} P_m(d_1)P\left(\|h_{u1}\|^2 < \frac{\eta}{N_m}\left(I_1 + \sigma_1^2\right)|d_1, m\right)\right\}. \end{aligned} \tag{15}$$

Since the probability of LOS link is related to the distance d_1, the conditional probability with a fixed d_1 and m will be firstly solved as,

$$\begin{aligned} &P\left(\|h_{u1}\|^2 < \frac{\eta}{N_m}\left(I_1 + \sigma_1^2\right)|d_1, m\right) \\ &\overset{(a)}{=} 1 - \sum_{J=0}^{N-1}\frac{1}{j!}\left(\eta\left(I_1 + \sigma_1^2\right)^j\right)e^{-\eta\left(I_1+\sigma_1^2\right)} \\ &\overset{(b)}{=} 1 - \sum_{J=0}^{N-1}\frac{(-\eta)^j}{j!}\left(e^{-\eta\left(I_1+\sigma_1^2\right)}\right)^{(j)}, \end{aligned} \tag{16}$$

where step-(a) is due to the cumulative distribution function of $\|h_{u1}\|^2$. And the j in the upper right corner of the step-(b) represents the j-th derivative of the formula.

Because the users are randomly and uniformly distributed in the cellular of radius R and satisfy $d_1 < d_2$, the pdf of d_1 and d_2 can be given by $f_{d_1}(r) = \frac{4}{R^2}r - \frac{4}{R^4}r^3$ and $f_{d_2}(r) = \frac{4}{R^4}r^3$, respectively, using order statistics. We set the $L(\eta) = e^{-\eta(I_1+\sigma_1^2)}$. By substituting (16) into (15), the item $P(\log(1+\gamma_{B1}) < R_1)$ can be denoted as

$$\begin{aligned} &P(\log(1+\gamma_{B1}) < R_1) \\ &= \mathbb{E}_{d_1}\left\{\sum_{m\in\{L,N\}} P_m(d_1)\left(1-\sum_{J=0}^{N-1}\frac{(-\eta)^j}{j!}(L(\eta))^{(j)}\right)\right\} \\ &= \sum_{m\in\{L,N\}}\sum_{J=0}^{N-1}\int_0^R\left(1-P_m(r)\frac{(-\eta)^j}{j!}(L(\eta))^{(j)}\left(\frac{4}{R^2}r-\frac{4}{R^4}r^3\right)\right)\mathrm{d}r \end{aligned} \tag{17}$$

The Gaussian-Chebyshev approximation can be adopted to calculate the integral in (17). And we set $\theta_i = \cos(\frac{(2i-1)/pi}{2M})$, $r_i = \frac{R}{2}(\theta_i+1)$, where M is the parameter of the Gaussian-Chebyshev approximation. Finally we can get the final expression,

$$\begin{aligned} P(\log(1+\gamma_{B1}) < R_1) = &\sum_{m\in\{L,N\}}\sum_{j=0}^{N-1}\sum_{i=1}^{M}\frac{R\pi\sqrt{1-\theta_i^2}}{2M} \\ &\times\left(1-P_m(r_i)\frac{(-\eta)^j}{j!}(L(\eta))^{(j)}f_{d_1}(r_i)\right). \end{aligned} \tag{18}$$

Similarly, the item $P(\log(1+\gamma_{U1}) < R_1)$ can also be derived using (18) by simply setting $\eta = \frac{\epsilon_2 L(d_1)N_m}{(\lambda_{LL(n)}\epsilon_1)P_n G(n)}$, $\epsilon_2 = 2^{R_2}-1$. Finally, P_1 can be derived by (12).

Next, we consider the outage probability of far user P_2. We set $\epsilon_3 = 2^{R_3}-1$, then the outage probability P_2 can be formulated as

$$\begin{aligned} P_2 &= P\left(\frac{\lambda_{UL(n)}G(n)P_n/L(d_2)\|h_{u2}\|^2}{\lambda_{LL(n)}G(n)P_n/L(d_2)\|h_{u2}\|^2+\sigma_2^2}\right. \\ &\qquad \left.+\frac{P_D/L(d_2-d_1)\left\|h_{I_D}\right\|^2}{\lambda_{LL(n)}G(n)P_n/L(d_2)\|h_{u2}\|^2+\sigma_2^2} < \epsilon_3\right) \\ &= P\left(\left\|h_{I_D}\right\|^2 < \frac{\beta}{N_m}(I_2-\xi)\right), \end{aligned} \tag{19}$$

where

$$\begin{cases} \beta = \left(\epsilon_3\lambda_{LL(n)}-\lambda_{UL(n)}\right)\frac{G(n)P_nL(d_2-d_1)}{L(d2)P_D} \\ \xi = \frac{L(d_2)\epsilon_3\sigma_2^2}{(\lambda_{UL(n)}-\epsilon_3\lambda_{LL(n)})G(n)P_n} \\ I_2 = \|h_{u2}\|^2. \end{cases} \tag{20}$$

The outage probability of far user can be calculated as

$$\begin{aligned} P_2 &= \mathbb{E}_{d_1,d_2,I_2}\left\{\sum_{m\in\{L,N\}}P_m(d_2)P\left(\left\|h_{I_D}\right\|^2<\frac{\beta}{N_m}(I_2-\xi)|d_1,d_2,m\right)\right\} \\ &= \sum_{m\in\{L,N\}}\sum_{j=0}^{N-1}\mathbb{E}_{d_1,d_2,I_2}\left\{1-P_m(d_2)\frac{(-\beta)^j}{j!}\left(e^{-\beta(I_2-\xi)}\right)^{(j)}\right\}. \end{aligned} \tag{21}$$

With the different values of system parameters, β can be divided into two cases to discuss. When $\beta > 0$, the $\epsilon\lambda_{LL}-\lambda_{UL} > 0$, the $P_1 = 1$. It means that the near user can not receive the broadcast signals all the time. In our actual deployment, we need to satisfy the formula $\epsilon\lambda_{LL}-\lambda_{UL} < 0$ between the power allocation ratio and the broadcast target rate to communicate properly.

When $\beta < 0$, if $I_2 \geq \xi$, $P_2 = 0$. And if $I_2 < \xi$, the P_2 can be formulated as,

$$\begin{aligned} \mathbb{E}_{I_2}\left\{e^{-\beta I_2}\right\} &= \int_0^{\xi}e^{-\beta x}\frac{N_m^{N_m}}{\Gamma(N_m)}x^{N_m-1}e^{-N_m x}dx \\ &= \frac{N_m^{N_m}}{\Gamma(N_m)}e^{-(N+\beta)\xi}\left(\sum_{k=0}^{N-1}\frac{(-1)k!\binom{N-1}{k}}{(N+\beta)^{k+1}}\xi^{N-1-k}\right) \\ &\quad+\left(1+\frac{\beta}{N_m}\right)^{-N_m} \end{aligned} \tag{22}$$

Next, the pdf of d_1 and d_2 can be used to calculated the expectation of d_1 and d_2, which is denoted as $f_{d_1,d_2}(r_1.r_2) = \frac{8r_1r_2}{R^4}$. We set the $L(\beta,\xi) = e^{\beta\xi}\mathbb{E}_{I_2}\{e^{-\beta I_2}\}$. We can get

$$\begin{aligned} P_2 &= \sum_{m\in\{L,N\}}\sum_{j=0}^{N-1}\mathbb{E}_{d_1,d_2}\left\{1-P_m(d_2)\frac{(-\beta)^j}{j!}(L(\beta,\xi))^{(j)}\right\} \\ &= \sum_{m\in\{L,N\}}\sum_{j=0}^{N-1}\int_0^R\int_0^{r_2}\left(1-P_m(r_2)\frac{(-\beta)^j}{j!}(L(\beta,\xi))^{(j)}\right. \\ &\qquad\left.\times f_{d_1,d_2}(r_1,r_2)\right)\mathrm{d}r_1\mathrm{d}r_2 \end{aligned} \tag{23}$$

Finally, we use Gaussian-Chebyshev approximation to calculate the integral (23). We define the parameters related to this approximation as follows:

$$\begin{cases} \theta_{1i} = \cos\left(\frac{(2i-1)\pi}{2M}\right) \\ r_{1i} = \frac{r_2}{2}(\theta_{1i}+1) \\ \theta_{2k} = \cos\left(\frac{(2k-1)\pi}{2M}\right) \\ r_{2k} = \frac{R}{2}(\theta_{2k}+1), \end{cases} \tag{24}$$

where M is the parameter of the Gaussian-Chebyshev approximation. The colosed-form expression of P_2 can be finally given by,

$$\begin{aligned} P_2 = &\sum_{m\in\{L,N\}}\sum_{j=0}^{N-1}\sum_{i=1}^{M}\sum_{k=1}^{M}\frac{R\pi}{2M}\sqrt{1-\theta_{2k}^2}\frac{r_{2k}\pi}{2M}\sqrt{1-\theta_{1i}^2} \\ &\times\left(1-P_m(r_{2k})\frac{\left(-\beta_{i,k}\right)^j}{j!}\left(L_{i,k}(\beta,\xi)\right)^{(j)}\right)f_{d_1,d_2}(r_{1i},r_{2k}). \end{aligned} \tag{25}$$

B. Ergodic Capacity

In the following, we analyse the ergodic capacity of two users which represents the ability of the entire system to deliver information. The ergodic capacity of the system,

denoted as C_{Erg}, can be obtained by Shannon's Law,

$$\begin{aligned} C_{\mathrm{Erg}} &= \mathbb{E}\big[\log_2(1+\gamma_{U_1})\big]+\mathbb{E}\big[\log_2(1+\gamma_{B_2})\big] \\ &= \mathbb{E}\left[\log_2\left(1+\frac{\lambda_{LL(n)}G(n)P_n/L(d_1)\|h_{u1}\|^2}{P_D/L_{I_1}\left\|h_{I_1}\right\|^2+\sigma_1^2}\right]\right. \\ &\quad \left.+\ \mathbb{E}\left[\log_2\left(1+\frac{\lambda_{UL(n)}G(n)P_n/L(d_2)\|h_{u2}\|^2+P_D/L(d_2-d_1)\left\|h_{I_D}\right\|^2}{\lambda_{LL(n)}G(n)P_n/L(d_2)\|h_{u2}\|^2+\sigma_2^2}\right)\right]\right. \end{aligned} \tag{26}$$

According to the literature [43], the capacity formula can be approximated by.

$$\mathbb{E}[\ln(1+x)] \approx \ln(1+\mathbb{E}[x]) - \frac{\mathbb{E}\big[x^2\big]-(\mathbb{E}[x])^2}{2(1+\mathbb{E}[x])^2}, \tag{27}$$

which reveals that the ergodic capacity can be approximated by a composite function of $\mathbb{E}[x]$ and $\mathbb{E}[x^2]$. Therefore, the following part focus on the derivation of $\mathbb{E}[x]$ and $\mathbb{E}[x^2]$.

Then we solve numerator part of the second item in Equation (26).

$$\begin{aligned} &\mathbb{E}_{h_{u2},h_{I_D},d1,d2}[x] \\ &= \mathbb{E}_{h_{u2},h_{I_D},d1,d2}\Big[G(n)P_n/\Big(L(d_2)\sigma_2^2\Big)\|h_{u2}\|^2 \\ &\qquad + P_D/\Big(L(d_2-d_1)\sigma_2^2\Big)\left\|h_{I_D}\right\|^2\Big] \\ &= \mathbb{E}_{d1,d2}\left[\sum_{u_2\in\{L,N\}} P_{u_2}(d_2)\left(G(n)\frac{P_n}{L(d_2)\sigma_2^2}+\frac{P_D}{L(d_2-d_1)\sigma_2^2}\right)\right] \\ &= \sum_{u_2\in\{L,N\}}\int_0^R\int_0^{r_2} P_{u_2}(r_2)L(r_1,r_2)f_{d_1,d_2}(r_1,r_2)\mathrm{d}r_1\mathrm{d}r_2, \end{aligned} \tag{28}$$

where $a = G(n)P_n/\sigma_2^2$ and $b = P_D/\sigma_2^2$. The term $L(r_1, r_2) = \frac{a}{r_2^{\alpha_{u_2}}} + \frac{b}{(r_2-r_1)^{\alpha_{I_D}}}$. The Gaussian-Chebyshev approximation can be also adopted to calculate the integral in (28). By setting (24), where M is the parameter of the Gaussian-Chebyshev approximation, we can derive $\mathbb{E}[x]$ as followed,

$$\begin{aligned} \mathbb{E}[x] = &\sum_{u_2\in\{L,N\}}\sum_{m=1}^{M}\sum_{i=1}^{M}\Big(\frac{\pi}{2M}\Big)^2\sqrt{1-\theta_i^2}R\sqrt{1-\theta_m^2}r_m \\ &\times P_{u_2}(r_m)L(r_i,r_m)f_{d_1,d_2}(r_{1i},r_{2m}). \end{aligned} \tag{29}$$

Next, $\mathbb{E}[x^2]$ is calculated by firstly solving the expectation of $\|h_{u2}\|^2$ and $\|h_{I_D}\|^2$, and then solving the expectation with respect to d_1, d_2 as follows,

$$\begin{aligned} &\mathbb{E}_{h_{u2},h_{I_D},d1,d2}\Big[x^2\Big] \\ &= \mathbb{E}_{h_{u2},h_{I_D},d1,d2}\Big[\Big(G(n)P_n/\Big(L(d_2)\sigma_2^2\Big)\|h_{u2}\|^2 \\ &\qquad + P_D/\Big(L(d_2-d_1)\sigma_2^2\Big)\left\|h_{I_D}\right\|^2\Big)^2\Big] \\ &= \sum_{u_2\in\{L,N\}}\int_0^R\int_0^{r_2} P_{u_2}(r_2)L(r_1,r_2)f_{d_1,d_2}(r_1,r_2)\mathrm{d}r_1\mathrm{d}r_2, \end{aligned} \tag{30}$$

where $c = G(n)P_n/\sigma_2^2$, $d = P_D/\sigma_2^20$. $L(r_1, r_2) = (\frac{c}{r_2^{\alpha_{u_2}}})^2(N_{u2}+1)/N_{u2} + (\frac{d}{(r_2-r_1)^{\alpha_{I_D}}})^2(N_{I_D}+1)/N_{I_D} + 2\cdot\frac{c}{r_2^{\alpha_{u_2}}}\cdot\frac{d}{(r_2-r_1)^{\alpha_{I_D}}}$. By setting (24), where M is the parameter of the Gaussian-Chebyshev approximation, we can derive $\mathbb{E}[x]$ as followed,

$$\begin{aligned} \mathbb{E}\Big[x^2\Big] = &\sum_{u_2\in\{L,N\}}\sum_{m=1}^{M}\sum_{i=1}^{M}\Big(\frac{\pi}{2M}\Big)^2\sqrt{1-\theta_i^2}R\sqrt{1-\theta_m^2}r_m \\ &\times P_{u_2}(r_m)L(r_i,r_m)f_{d_1,d_2}(r_{1i},r_{2m}). \end{aligned} \tag{31}$$

By substituting (29) and (31) into (27), the numerator part of the second item in equation (26) can be calculated. The first item in equation (26) is

$$\mathbb{E}\left[\log_2\left(1+\frac{\lambda_{LL(n)}G(n)P_n/L(d_1)\|h_{u1}\|^2}{P_D/L_{I_1}\left\|h_{I_1}\right\|^2+\sigma_1^2}\right)\right]. \tag{32}$$

We set $a = \frac{\lambda_{LL(n)}G(n)P_n}{P_D/L_{I_1}\|h_{I_1}\|^2+\sigma_1^2}$. Similar to the (29) and (31), the $\mathbb{E}[x]$ and $\mathbb{E}[x^2]$ should be calculated first. Then we can get

$$\mathbb{E}[x] = \sum_{u_2\in\{L,N\}}\sum_{i=1}^{M}\Big(\frac{\pi}{2M}\Big)R\sqrt{1-\theta_i^2}P_{u_1}(r_i)L(r_i)f_{d_1}(r_i), \tag{33}$$

where $L(r_i) = 1/(r)^{\alpha_{u_1}}$.

$$\mathbb{E}\Big[x^2\Big] = \sum_{u_2\in\{L,N\}}\sum_{i=1}^{M}\Big(\frac{\pi}{2M}\Big)R\sqrt{1-\theta_i^2}P_{u_1}(r_i)L(r_i)f_{d_1}(r_i), \tag{34}$$

where $L(r_i) = (N_{u1}+1)/(N_{u1}(r)^{2\alpha_{u_1}})$.

Then we can submit (33) and (34) into (27) to calculate the first item in equation (26). As for the Denominator of the second item in equation (26), we only change the value of a of (33) and (34). Finally, we combine all the item in the equation (26), and the ergodic capacity can be obtained in a closed-form.

IV. Numerical Results

In this section, the outage probability and the ergodic capacity of the beamspace MIMO-NOMA millimeter wave broadcasting network via full-duplex D2D communications are investigated. The impact of the transmission power of base station, the antenna number of base station, the transmission power of near user and the power allocation on the outage probability and ergodic capacity are introduced as followed. The traditional TDM scheme without D2D communications and the LDM without D2D communications are used for comparison to analyze the performance of the proposed system. In particular, the time slot is equally divided by the two users. Hence the capacity of this scheme is R_{TDM}, which is denoted as

$$R_{TDM} = \frac{1}{2}(\log(1+\gamma_1)+\log(1+\gamma_2)). \tag{35}$$

The numerical results of the proposed system performance are considered with Monte Carlo simulations. The simulation parameters and setting of the proposed system are shown at Table I.

TABLE I
THE SIMULATION PARAMETERS AND SETTING OF THE PROPOSED SYSTEM

Parameter	Value
Carrier frequency	28GHz
Bandwidth	200MHz
Coverage radius	30
The number of base station antenna	64
The transmission power of the near user	5dbm
The isolation of the transmitted and received in the near user	125dB
The power coefficient of the LDM	0.15
The small scale fading N_L	2
The small scale fading N_N	3
The pass loss exponents α_L	2
The pass loss exponents α_N	3
The blockage parameter	0.001
The target rate R_1	3.8bit/s/Hz
The target rate R_2	10bit/s/Hz
The target rate R_3	3.8bit/s/Hz

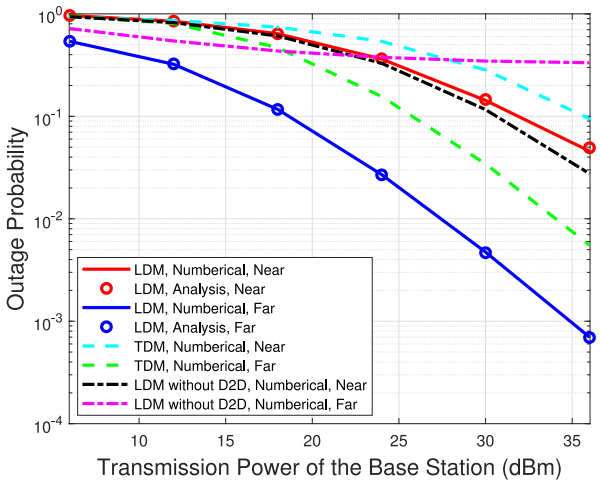

Fig. 3. Impact of the base station transimission power on outage probability.

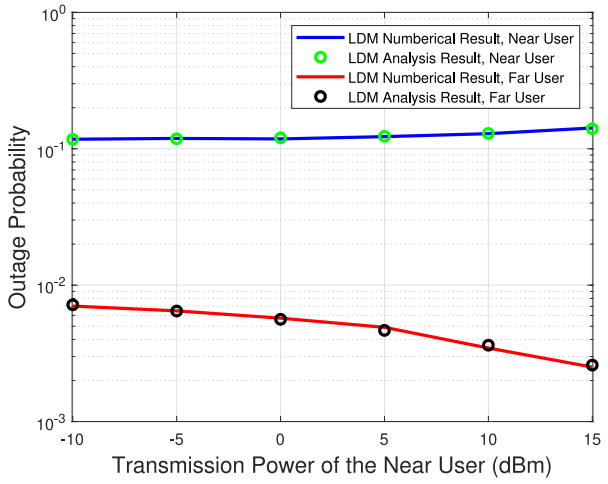

Fig. 4. Impact of the near user transimission power on outage probability.

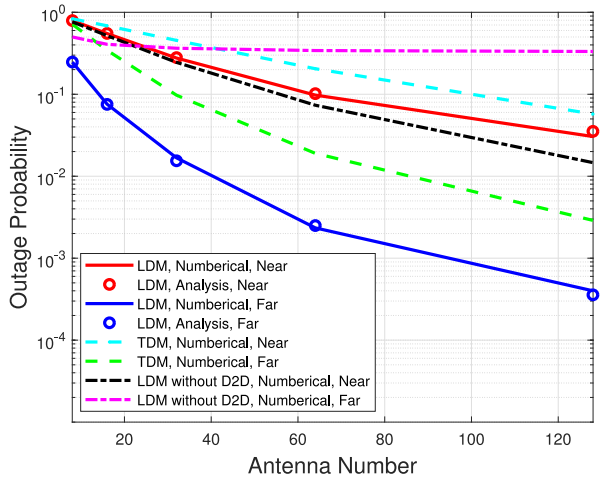

Fig. 5. Impact of the antenna number on outage probability.

A. *Outage Probability*

The outage probability of the near user and the far user are analysed in this section.

In Fig. 3, the impacts of the base station transmission power on the outage probability are analysed. It can be seen from the figure that the Monte Carlo simulation is consistent with the proposed closed-formed expression. With the increasing of the transmission power of base station, the outage probability of near user and far user are decreasing, where the LDM outperforms the traditional TDM mode. In addition, compared with LDM without D2D, the outage probability of the near user increases slightly, but the outage probability of the far user decrease by 30 dB. Hence, increasing the transmission power of base station can be considered to reduce the outage probability further to enlarge the coverage and enhance the throughput of the whole system.

In Fig. 4, due to the self-interference of the near user, the outage probability of the near user slightly increase with the transmission power of the near user increasing. In addition, the outage probability of far user keeps a downward tendency which benefits from the improvement of the SNR at the receiving end of the D2D communication. The SNR went from -10 dB to 15 dB and the outage probability of far user dropped by about half. In the practical application, the transmission power of the near user can be increased with a small impact on the near user to reduce the outage probability of the far user and further to enhance the cellular coverage.

In Fig. 5, the effect of the antenna number of base station on the outage probability is considered. The simulation results verify that the large scale antenna arrays have a obvious affection on the outage probability at the mmWave MIMO-NOMA broadcasting network. The outage probability of the proposed LDM is 10 dB lower than the TDM. In actual system deployment, a large scale antenna arrays is adopted to compensate for the problem of large attenuation of millimeter wave in signal transmission, which can improve the transmission rate of the system, reduce delay and ameliorate the QoS.

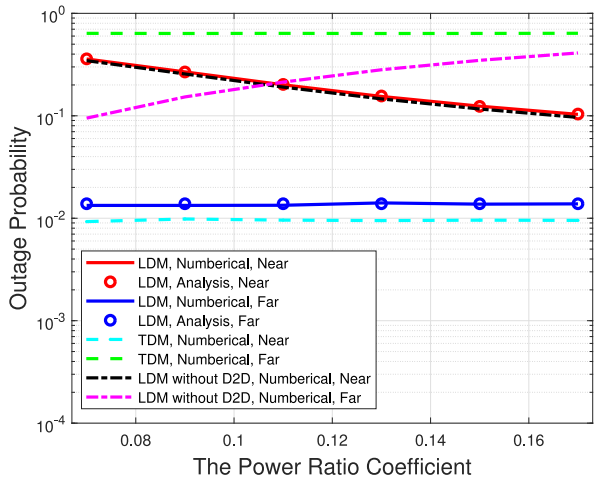

Fig. 6. Impact of power ratio coefficient on outage probability.

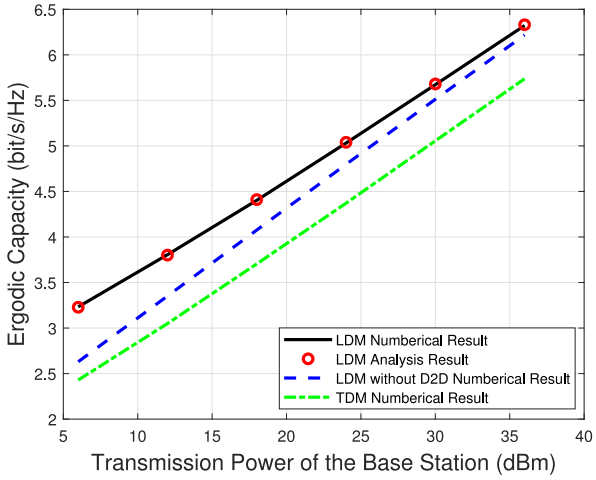

Fig. 7. Impact of the base station transimission power on ergodic capacity.

In Fig. 6, it has shown that power allocation has a greater impact on near user, because the lower layer is used to transmit unicast signals of the near user. When the power ratio is small, the outage probability increases. Moreover, far user not only receives signals from the base station, but also receives signals from the D2D link, so the impact is small. In order to reduce the outage probability of near user, the power ratio coefficient can be appropriately increased.

Simulation results show that the performance of LDM is better than the TDM. It can be seen that the non-orthogonal multiple access method can achieve high spectrum efficiency and high throughput wireless transmission services by slightly increasing the complexity of the receiver while the hardware transmission structure is unchanged. In addition, it can be seen that the transmission power and the number of antennas of the base station can be increased to reduce the outage probability.

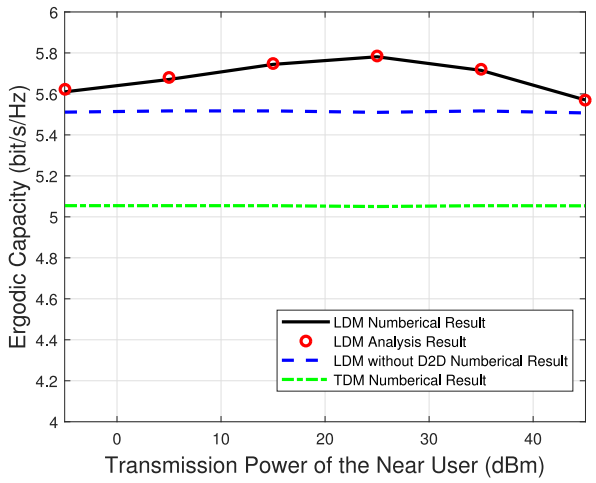

Fig. 8. Impact of the near user transimission power on ergodic capacity.

B. Ergodic Capacity

In this section, the ergodic capacity of the proposed system which is the sum rate of the near user and the far user is considered. Four factors such as the transmission power of the base station, the transmission power of the near user, the number of antenna and the power allocation are analysed as followed.

In Fig. 7, the impact of base station transmission power on the ergodic capacity is investigated. It can be seen that the simulation results match to the closed form expression of the proposed LDM which is better than the TDM and the LDM without D2D communications. In addititon, the ergodic capacity is approximately linearly related to the transmission power of the base station. The ergodic capacity of the proposed LDM is about 1.2 bit/s/Hz higher than the TDM. In the actual deployment, increasing the transmission power of the base station as much as possible to enlarge the coverage and improve the throughput of the entire system under the actual constrains such as human safety, power consumption and heat dissipation, etc.

In Fig. 8, it is shown that as the transmission power of the near user increasing, the ergodic capacity increases first, and decrease next. When the transmission power of the near user is small, the self-interference of the near user has little effect on the system ergodic capacity. At this time, the decisive factor for the total system ergodic capacity is the capacity of the far user. The capacity of the far user increases with the transmission power of the near user increasing. However, when the transmission power of the near user is large, the self-interference becomes an important factor affecting the system capacity. Therefore, in actual deployment, multiple aspects of the entire system must be fully considered to determine the transmission power of the near user to ensure the maximum system ergodic capacity. First, the parameters of the cellular network can be fixed. Then we can use the power of full-duplex transmission link as a variable to derive the system capacity of the cellular network, and make the derivative equal to zero. Finally, the optimal transmission power can be adopted.

In Fig. 9, the system ergodic capacity increases in logarithmic form as the number of antennas increases. Meanwhile, the simulation results indicates that the ergodic capacity of LDM is improved better than the TDM. The proposed LDM

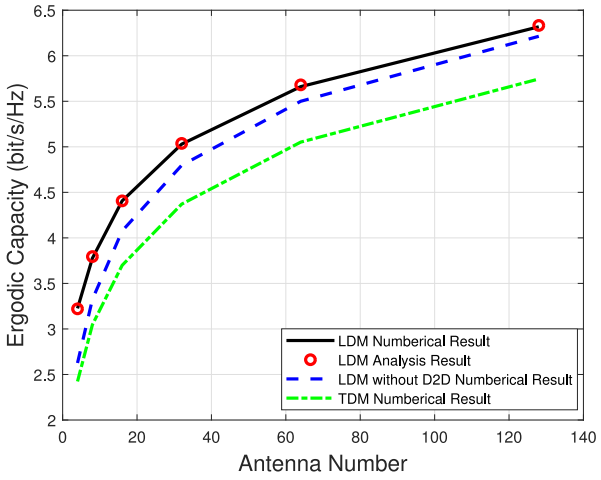

Fig. 9. Impact of the antenna number on ergodic capacity.

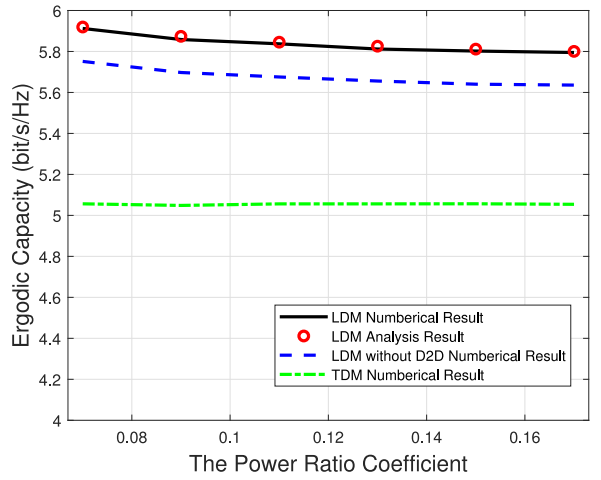

Fig. 10. Impact of power ratio coefficient on ergodic capacity.

is 0.2 bit/s/Hz higher than the LDM without D2D communications when the antenna number larger than 64. The millimeter wave is easy to integrate large scale antenna arrays thanks to its short wavelength. In addition, we need to make a trade-off between the increments of the system capacity and the power consumption of the large scale antennas and radio frequency chains.

In Fig. 10, when the power factor changes, the ergodic capacity remains almost unchanged. Meanwhile, the simulation results indicates that the ergodic capacity of the proposed LDM is improved better than the TDM and the LDM without D2D communications.

The impact factors of the system ergodic capacity are considered. The system ergodic capacity will increase with the transmission power of base station and the antenna number of base station increasing. Furthermore, the transmission power of the near user should be optimized to enlarge the system ergodic capacity.

V. Conclusion

In this paper, the outage probability and the ergodic capacity of the mmWave MIMO-NOMA broadcasting network with full-duplex D2D communications are presented. The accuracy of the analysis is then verified by detailed numerical results. Compared with the conventional TDM-based and LDM without D2D scheme, our proposed scheme achieves significant performance gains with respect to both outage probability and the ergodic capacity. We also observe that the system performance can be improved with higher transmission power and the larger antenna array at the base station. Besides, the transmission power of the full-duplex communication should be optimized to ensure low self-interference and large capacity.

References

[1] L. Fay, L. Michael, D. Gómez-Barquero, N. Ammar, and M. W. Caldwell, "An overview of the ATSC 3.0 physical layer specification," *IEEE Trans. Broadcast.*, vol. 62, no. 1, pp. 159–171, Mar. 2016.

[2] Y. Wu, B. Rong, K. Salehian, and G. Gagnon, "Cloud transmission: A new spectrum-reuse friendly digital terrestrial broadcasting transmission system," *IEEE Trans. Broadcast.*, vol. 58, no. 3, pp. 329–337, Sep. 2012.

[3] B. Rong, Y. Qian, K. Lu, H. Chen, and M. Guizani, "Call admission control optimization in WIMAX networks," *IEEE Trans. Veh. Technol.*, vol. 57, no. 4, pp. 2509–2522, Jul. 2008.

[4] F. Hartung, U. Horn, J. Huschke, M. Kampmann, T. Lohmar, and M. Lundevall, "Delivery of broadcast services in 3G networks," *IEEE Trans. Broadcast.*, vol. 53, no. 1, pp. 188–199, Mar. 2007.

[5] D. Gómez-Barquero, D. Navratil, S. Appleby, and M. Stagg, "Point-to-multipoint communication enablers for the fifth generation of wireless systems," *IEEE Commun. Stand. Mag.*, vol. 2, no. 1, pp. 53–59, Mar. 2018.

[6] N. Ye, X. Li, H. Yu, L. Zhao, W. Liu, and X. Hou, "DeepNOMA: A unified framework for noma using deep multi-task learning," *IEEE Trans. Wireless Commun.*, early access, doi: 10.1109/TWC.2019.2963185.

[7] J. Zhao, O. Simeone, D. Gündüz, and D. Gómez-Barquero, "Non-orthogonal unicast and broadcast transmission via joint beamforming and LDM in cellular networks," *IEEE Trans. Broadcast.*, early access.

[8] N. Ye, H. Han, L. Zhao, and A.-H. Wang, "Uplink nonorthogonal multiple access technologies toward 5G: A survey," *Wireless Commun. Mobile Comput.*, vol. 2018, Jun. 2018, Art. no. 6187580.

[9] B. Xiao, K. Xiao, Z. Chen, B. Xia, and H. Liu, "Joint design for modulation and constellation labels in multiuser superposition transmission," *IEEE Trans. Broadcast.*, vol. 65, no. 2, pp. 245–259, Jun. 2019.

[10] J. An, K. Yang, J. Wu, N. Ye, S. Guo, and Z. Liao, "Achieving sustainable ultra-dense heterogeneous networks for 5G," *IEEE Commun. Mag.*, vol. 55, no. 12, pp. 84–90, Dec. 2017.

[11] K. Yang, N. Yang, N. Ye, M. Jia, Z. Gao, and R. Fan, "Non-orthogonal multiple access: Achieving sustainable future radio access," *IEEE Commun. Mag.*, vol. 57, no. 2, pp. 116–121, Feb. 2019.

[12] N. Ye, X. Li, H. Yu, A. Wang, W. Liu, and X. Hou, "Deep learning aided grant-free NOMA toward reliable low-latency access in tactile Internet of Things," *IEEE Trans. Ind. Informat.*, vol. 15, no. 5, pp. 2995–3005, May 2019.

[13] N. Ye, A. Wang, X. Li, W. Liu, X. Hou, and H. Yu, "On constellation rotation of NOMA with SIC receiver," *IEEE Commun. Lett.*, vol. 22, no. 3, pp. 514–517, Mar. 2018.

[14] L. Zhang *et al.*, "Layered-division-multiplexing: Theory and practice," *IEEE Trans. Broadcast.*, vol. 62, no. 1, pp. 216–232, Mar. 2016.

[15] S. I. Park *et al.*, "Low complexity layered division multiplexing system for the next generation terrestrial broadcasting," in *Proc. IEEE Int. Symp. Broadband Multimedia Syst. Broadcast.*, Jun. 2015, pp. 1–3.

[16] J. Montalban *et al.*, "Asynchronous N-layered division multiplexing (N-LDM)," in *Proc. IEEE Int. Symp. Broadband Multimedia Syst. Broadcast. (BMSB)*, Jun. 2016, pp. 1–6.

[17] J. Montalban *et al.*, "Performance study of layered division multiplexing based on SDR platform," *IEEE Trans. Broadcast.*, vol. 61, no. 3, pp. 436–444, Sep. 2015.

[18] L. Zhang, Y. Wu, G. K. Walker, W. Li, K. Salehian, and A. Florea, "Improving LTE *e* MBMS with extended OFDM parameters and layered-division-multiplexing," *IEEE Trans. Broadcast.*, vol. 63, no. 1, pp. 32–47, Mar. 2017.

[19] E. Garro, J. J. Gimenez, S. I. Park, and D. Gómez-Barquero, "Layered division multiplexing with multi-radio-frequency channel technologies," *IEEE Trans. Broadcast.*, vol. 62, no. 2, pp. 365–374, Jun. 2016.

[20] Z. Zhang, Z. Ma, M. Xiao, Z. Ding, and P. Fan, "Full-duplex device-to-device-aided cooperative nonorthogonal multiple access," *IEEE Trans. Veh. Technol.*, vol. 66, no. 5, pp. 4467–4471, May 2017.

[21] H. V. Vu, N. H. Tran, and T. Le-Ngoc, "Full-duplex device-to-device cellular networks: Power control and performance analysis," *IEEE Trans. Veh. Technol.*, vol. 68, pp. 3952–3966, Apr. 2019.

[22] I. Krikidis, H. A. Suraweera, S. Yang, and K. Berberidis, "Full-duplex relaying over block fading channel: A diversity perspective," *IEEE Trans. Wireless Commun.*, vol. 11, pp. 4524–4535, Dec. 2012.

[23] M.-K. Byun, D. Park, and B. G. Lee, "Performance and distance spectrum of space-time codes in fast Rayleigh fading channels," *IEEE Trans. Commun.*, vol. 56, no. 12, pp. 2105–2115, Dec. 2008.

[24] L. Jiménez Rodríguez, N. H. Tran, and T. Le-Ngoc, "Performance of full-duplex AF relaying in the presence of residual self-interference," *IEEE J. Sel. Areas Commun.*, vol. 32, no. 9, pp. 1752–1764, Sep. 2014.

[25] G. Liu, W. Feng, Z. Han, and W. Jiang, "Performance analysis and optimization of cooperative full-duplex D2D communication underlaying cellular networks," *IEEE Trans. Wireless Commun.*, vol. 18, no. 11, pp. 5113–5127, Nov. 2019.

[26] H. Chour, Y. Nasser, O. Bazzi, and F. Bader, "Full-duplex or half-duplex D2D mode? Closed form expression of the optimal power allocation," in *Proc. 25th Int. Conf. Telecommun. (ICT)*, Jun. 2018, pp. 498–504.

[27] W. Chang and J. Teng, "Energy efficient relay matching with bottleneck effect elimination power adjusting for full-duplex relay assisted D2D networks using mmWave technology," *IEEE Access*, vol. 6, pp. 3300–3309, 2018.

[28] Y. Wang, Y. Niu, H. Wu, Z. Han, B. Ai, and Q. Wang, "Sub-channel allocation for device-to-device underlaying full-duplex mmWave small cells using coalition formation games," *IEEE Trans. Veh. Technol.*, vol. 68, no. 12, pp. 11915–11927, Dec. 2019.

[29] B. Ma, H. Shah-Mansouri, and V. W. S. Wong, "Full-duplex relaying for D2D communication in millimeter wave-based 5G networks," *IEEE Trans. Wireless Commun.*, vol. 17, no. 7, pp. 4417–4431, Jul. 2018.

[30] R. T. Schwarz, T. Delamotte, K. Storek, and A. Knopp, "MIMO applications for multibeam satellites," *IEEE Trans. Broadcast.*, vol. 65, no. 4, pp. 664–681, Dec. 2019.

[31] W. Hong, K.-Y. Baek, Y. Lee, Y. Kim, and S.-T. Ko, "Study and prototyping of practically large-scale mmWave antenna systems for 5G cellular devices," *IEEE Commun. Mag.*, vol. 52, no. 9, pp. 63–69, Sep. 2014.

[32] B. Yang, Z. Yu, J. Lan, R. Zhang, J. Zhou, and W. Hong, "Digital beamforming-based massive MIMO transceiver for 5G millimeter-wave communications," *IEEE Trans. Microw. Theory Techn.*, vol. 66, no. 7, pp. 3403–3418, Jul. 2018.

[33] J. G. Andrews, T. Bai, M. N. Kulkarni, A. Alkhateeb, A. K. Gupta, and R. W. Heath, "Modeling and analyzing millimeter wave cellular systems," *IEEE Trans. Commun.*, vol. 65, no. 1, pp. 403–430, Jan. 2017.

[34] X. Gao, D. Niyato, P. Wang, K. Yang, and J. An, "Contract design for time resource assignment and pricing in backscatter-assisted RF-powered networks," *IEEE Wireless Commun. Lett.*, vol. 9, no. 1, pp. 42–46, Jan. 2020.

[35] X. Gao, P. Wang, D. Niyato, K. Yang, and J. An, "Auction-based time scheduling for backscatter-aided RF-powered cognitive radio networks," *IEEE Trans. Wireless Commun.*, vol. 18, no. 3, pp. 1684–1697, Mar. 2019.

[36] Z. Wang, Q. Liu, M. Li, and W. Kellerer, "Energy efficient analog beamformer design for mmWave multicast transmission," *IEEE Trans. Green Commun. Netw.*, vol. 3, no. 2, pp. 552–564, Jun. 2019.

[37] B. Wang, L. Dai, Z. Wang, N. Ge, and S. Zhou, "Spectrum and energy-efficient beamspace MIMO-NOMA for millimeter-wave communications using lens antenna array," *IEEE J. Sel. Areas Commun.*, vol. 35, no. 10, pp. 2370–2382, Oct. 2017.

[38] J. Jin, C. Xiao, W. Chen, and Y. Wu, "Hybrid precoding in mmWave MIMO broadcast channels with dynamic subarrays and finite-alphabet inputs," in *Proc. IEEE Int. Conf. Commun. (ICC)*, May 2018, pp. 1–6.

[39] T. Bai and R. W. Heath, "Coverage and rate analysis for millimeter-wave cellular networks," *IEEE Trans. Wireless Commun.*, vol. 14, no. 2, pp. 1100–1114, Feb. 2015.

[40] S. A. R. Naqvi and S. A. Hassan, "Combining NOMA and mmWave technology for cellular communication," in *Proc. IEEE 84th Veh. Technol. Conf. (VTC-Fall)*, Sep. 2016, pp. 1–5.

[41] Y. Sun, Z. Ding, and X. Dai, "On the performance of downlink NOMA in multi-cell mmWave networks," *IEEE Commun. Lett.*, vol. 22, no. 11, pp. 2366–2369, Nov. 2018.

[42] N. Deng and M. Haenggi, "A fine-grained analysis of millimeter-wave device-to-device networks," *IEEE Trans. Commun.*, vol. 65, no. 11, pp. 4940–4954, Nov. 2017.

[43] Y. Huang, F. Al-Qahtani, C. Zhong, Q. Wu, J. Wang, and H. Alnuweiri, "Performance analysis of multiuser multiple antenna relaying networks with co-channel interference and feedback delay," *IEEE Trans. Commun.*, vol. 62, no. 1, pp. 59–73, Jan. 2014.